COMPDYN 2025
10th ECCOMAS Thematic Conference on
Computational Methods in Structural Dynamics and Earthquake Engineering
M. Papadrakakis, M. Fragiadakis (eds.)
Rhodes Island, Greece, 15-18 June 2025

TOWARDS LOSS-BASED SEISMIC DESIGN FOR BRIDGES: ACCURACY OF SIMPLIFIED STRATEGIES FOR LOSS ASSESSMENT

Andrea Nettis[1], Roberto Gentile[2], Domenico Raffaele[1] and Giuseppina Uva[1]

[1] Department of Civil, Environmental, Land, Building Engineering and Chemistry
Polytechnic University of Bari, Bari, Italy
e-mail: {a.nettis, d.raffaele, g.uva}@poliba.it

[2] Department of Risk and Disaster Reduction, University College London, United Kingdom
e-mail: r.gentile@ucl.ac.uk

Abstract

Loss-based seismic design involves targeting selected levels of earthquake-induced loss (e.g., deaths, dollars, downtime). Achieving this in the practice, without resorting to tedious trial-and-error procedures, requires using simplified loss assessment strategies for a set of seed structures, thus selecting the one(s) complying with the selected loss target. As the first step towards practical loss-based design for bridges, this paper investigates the trade-off between simplicity (modelling effort and computational time) and result accuracy in the seismic loss analysis of reinforced concrete (RC) bridges. The study involves a set of 18 case-study bridges imagined in a high-seismicity site. For each of them, a benchmark estimation of the expected annual loss is obtained running non-linear time-history analyses of refined multi-degree of freedom models. Such estimates are obtained with alternative, simplified strategies including: 1) analytical non-linear static analyses (i.e., pseudo pushover) using the displacement-based assessment paradigm, coupled with the capacity spectrum method; 2) the same non-linear static analyses coupled with a surrogate probabilistic seismic demand model based on a Gaussian process regression. This sensitivity analysis also tests the impact of the assumed functional form for the probabilistic seismic demand model (power-law or a bilinear). Although the results are preliminary and potentially subjected to refinements, the use of the displacement-based pseudo pushover together with the capacity spectrum method shows the potential to be included in a practice-oriented loss-based design paradigm for bridges. Conversely, adopting a surrogate model-based loss-assessment would first require challenging some of its simplified assumptions.

Keywords: Losses, Seismic risk, Bridges, Displacement-based assessment, Nonlinear time history analysis, Capacity Spectrum Method

1 INTRODUCTION

Earthquake loss assessment involves computing a loss metric (e.g. deaths, dollars, downtime) for a fully specified asset configuration, with the most widely accepted framework being performance-based earthquake engineering (PBEE [1]). Loss assessment is a highly non-linear and uncertain mathematical problem considering, among many other factors, that the fragility module depends on non-linear time-history analyses (NLTHA). Conversely, loss-based design involves targeting an acceptable level of loss under a specified site hazard profile.

Since loss assessment is not invertible, most risk- or loss-based design procedures involve repeated applications of a loss assessment methodology while revising a guess design candidate until the target decision variable is met. This tends to be particularly demanding in computational effort and time. Such iterative approaches are arguably more appropriate for the advanced design stages than the conceptual or preliminary design phases. Direct procedures (e.g., [2]), arguably more suitable for preliminary design, require an explicit mathematical formulation (e.g. mapping a decision variable to key bridge design parameters). Given the complexity of the loss-assessment problem, this explicit mathematical mapping can be achieved only by accepting a trade-off between the simplicity of the adopted framework and the refinement of the solution [3].

As a first step towards non-iterative loss-based design of bridges, this paper provides a sensitivity analysis of alternative loss-assessment methodologies, analysing their simplicity-vs-accuracy trade-offs. This is done on a dataset of 18 case-study continuous-deck reinforced concrete (RC) bridges characterised by single-column piers imagined in a high-seismicity site. For such case studies, estimates of the expected annual loss (EAL) are obtained alternatively with two literature methodologies applied for fragility analysis (described in Section 2). Such estimates are compared with benchmark values obtained with a refined one based on non-linear time-history analyses. This paper aims at identifying, among the tested alternatives, a promising loss assessment methodology which is simplified enough to be adopted during the preliminary design phase and accurate enough to provide relevant insights for decision-making. More importantly, the discussion aims at identifying the gaps affecting the best-performing loss-assessment methodologies, and any further development required to overcome those before including it as part of a practical loss-based design paradigm.

2 METHODOLOGY

This section illustrates the methodologies adopted for loss assessment and for fragility analysis. It first presents the system-level loss assessment approach based on fragility relationships for various bridge damage states (DSs). Then, it details the fragility analysis methods, incorporating different seismic response strategies and functional forms for probabilistic seismic demand models.

2.1 Loss assessment

The estimation of expected losses for a given structure can be characterised by using a system-level approach (recommended in [4] and applied to bridges in [5, 6]), or in a component-by-component fashion (described in [7] and applied to bridges in [8]). The latter approach is the most refined and requires a more detailed input, while the former is simplified and it has been successfully included within existing loss-based design applications [2]. Therefore, the loss assessment procedure adopted in this study pertains to the system-level category. Direct economic losses associated with the repairing/replacement of a damaged bridge are considered in this study. Indirect losses (e.g., related to disruption time, variation of traffic flows within

the network and increasing travelling time for users) will be considered in further developments [9, 10].

In this study, the expected annual loss (EAL) is computed according to Equation (1), where $LR(IM)$ is the expected loss ratio (taken from a vulnerability model) and $H(IM)$ represents the hazard curve (i.e., the mean annual frequency of exceeding different values of the intensity measure, or IM).

$$EAL = \int LR(IM) \left| \frac{dH(IM)}{dIM} \right| dIM \tag{1}$$

The hazard curves are computed with specific reference to the location of the analysed structure by means of a probabilistic seismic hazard analysis. Expected loss ratio functions express direct losses as a ratio to the total cost of demolition and reconstruction conditioned to a given IM value. $LR(IM)$ are computed via Equation (2) in which P_{DS_k}(IM) represents the probability of the structure being in a given DS for a given IM and DLR_k are the damage-to-loss ratios, expressing the loss for a given DS normalised with respect to the total cost of reconstruction. P_{DS_k}(IM) is calculated based on fragility functions $F(DS|IM)$ via Equation (3) in which N_{DS} is the number of considered DSs. Fragility functions represent the probability of reaching or exceeding a given DSs and can be computed according to numerous existing procedures in the literature based on numerical simulations or post-earthquake observations.

$$LR(IM) = \sum_{k=1}^{N_{DS}} DLR_k \, P_{DS_k}(IM) \tag{2}$$

$$P_{DS_k}(IM) = \begin{cases} F_{DS_k}(IM) - F_{DS_{k+1}}(IM), & \mathrm{k} = 1, \dots, \mathrm{N}_{DS} - 1 \\ F_{DS_k}(IM), & \mathrm{k} = \mathrm{N_{DS}} \end{cases} \tag{3}$$

In this study, system-level fragility relationships are calculated for a set of structure-specific DSs according to cloud analysis [11]. $F_{DS}(IM)$ is expressed via Equation (4) and represent the conditional probability that the DS is reached or exceeded, i.e. a given engineering demand parameter (EDP) exceeds a given DS threshold conditioned to an IM value. The fragility relationship is calculated based on $[edp, im]_j$ observations generated by carrying out seismic response analyses adopting natural unscaled ground motions.

The elaboration of the $[edp, im]_j$ data leads to the computation of the conditional probability that the DS is reached, given that collapse does not occur, $P(DS|IM, NoC)$ and the probability of collapse $P(C|IM)$ [11]. The probability of collapse $P(C|IM)$ is fitted on the seismic response analysis dataset with a logistic regression, which is appropriate for cases in which the response variable is binary (‘‘collapsed’’ or ‘‘non-collapsed’’). Conversely, the computation of $P(DS|IM, NoC)$ requires the definition of the so-called probabilistic seismic demand model expressing the analytical relationships between EDP and IM in case of no collapse. The EDP is a generic structural demand parameter of interest (i.e., base cross-section curvature, drift or displacement of the piers), while the IM is a generic seismic intensity parameter (see [12]).

$$F_{DS}(IM) = \mathrm{P(DS|IM)} = \mathrm{P(DS|IM, NoC)}\big(1 - P(C|IM)\big) + P(C|IM)) \tag{4}$$

Two functional forms for probabilistic seismic demand models are considered in this study. The first is the power-law model, i.e. $\widehat{EDP} = aIM^b$. The parameters $[a, b]$ of the power model are estimated by fitting a linear model to the cloud data $[edp, im]_j$ transformed in the natural logarithmic scale, using the least square regression method. The dispersion σ of the EDP around the median estimated with the power-law model is assumed to be constant with respect to IM and is given by Equation (5) where M is the number of ground motions.

$$\sigma = \sqrt{\frac{\sum_{j=1}^{M}(\ln edp_j - \ln a(im_j)^b)}{M-2}} \tag{5}$$

The second considered functional form for probabilistic seismic demand model is based on a bilinear EDP-IM relationship. A short presentation on the use of the bilinear model is proposed as follows, however the readers can refer to [13] for in-depth clarifications.

This approach assumes an equivalent single-degree-of-freedom (SDoF) response of the analysed structure. First, the equivalent SDoF monotonic shear-displacement relationship of the analysed structure is computed and the coordinates of yielding point in terms of yielding shear ratio (f_y) and displacement are extracted, together with the secant-to-yielding period (T_{eff}). This strategy assumes the EDP is the equivalent SDoF displacement ductility (μ_{EDP}) and the IM reflects the ratio between the spectral acceleration (SA), computed at T_{eff}, and f_y and is represented by R_{IM}. Therefore, the cloud data should be converted as $[\mu_{EDP}, R_{IM}]_j$. The bilinear EDP-IM relationship is defined according to Equation (5). The first segment corresponds to the equivalent SDoF elastic response and does not require analysis results to be calibrated. The inelastic segment is obtained performing a linear regression in the logarithmic space, where $\sigma_{\ln(\hat{\mu}_{\mathrm{EDP}}-1)|R_{IM}-1} = \sigma$ is the logarithmic standard deviation of the observations $\mu_{EDP} - 1$ versus $R_{IM} - 1$ calculated via seismic response analyses, and ε is a standard normal variable. Therefore, the median relationship is $\hat{\mu}_{\mathrm{EDP}} = a(R_{IM} - 1) + 1$, where a is the slope of the linear inelastic branch of the bilinear model. Such a model choice implies a lognormal distribution of the residuals and homoscedasticity for $\mu_{EDP} > 1$.

$$\begin{cases} \hat{\mu}_{\mathrm{EDP}} = R & \hat{\mu}_{\mathrm{EDP}} \leq 1 \\ \ln(\hat{\mu}_{\mathrm{EDP}} - 1) = \ln(a) + \ln(R-1) + \varepsilon\sigma_{\ln(\hat{\mu}_{\mathrm{EDP}}-1)|R-1} & \hat{\mu}_{\mathrm{EDP}} > 1 \end{cases} \tag{6}$$

The conditional probability that the EDP threshold is exceeded, given that collapse does not occur is computed via Equation (7) in which $\phi(\cdot)$ the Normal cumulative distribution function. DS thresholds ($\mathrm{EDP_{DS}}$) should be expressed in terms of the EDP of interest. In case of a bilinear model is used $\mathrm{EDP_{DS}}$ should reflect equivalent SDoF ductility limits representative of the damage condition of the bridge.

$$P(DS|IM, NoC) = 1 - \phi\left(\frac{\ln \mathrm{EDP_{DS}} - \ln \widehat{\mathrm{EDP}}}{\sigma}\right) \tag{7}$$

2.2 Strategies for fragility analysis

In a bridge-level loss assessment, fragility functions are derived from a set of simulations of the seismic response under varying intensity of the seismic action. The most rigorous approach involves NLTHA of a detailed structural model using an extensive set of ground-motion records

([11, 14]). However, as mentioned in the introduction, for loss-/risk-based design, the use of NLTHA on many tentative structural candidates is unaffordable, motivating the need for using approximate fragility analysis methodologies.

The simplified strategies for loss assessment tested in this study are based on the use of nonlinear static procedures applying displacement-based assessment (DBA) algorithms. Those are aimed at computing equivalent SDoF force-displacement relationships of the investigated bridge. The DBA involves analytical calculations which can be performed by using simple programming routines and, therefore, could represent a suitable solution for analysing multiple tentative realisations of the structures in a loss-based design framework. Sadan et al. and Gentile et al. [15, 16] introduced the first versions of DBA for continuous-deck reinforced concrete (RC) multi-span bridges. For the seismic analysis of the bridge in the transverse direction, DBA algorithms use a simplified modelling approach in which the bridge is modelled by an equivalent elastic beam based on inelastic supports. The inelastic supports are assigned the equivalent cantilever force-displacement response of the substructure components (including the response of the bearing devices, shear keys, foundations). By means of iterative equivalent elastic analyses (i.e. eigenvalue analyses with secant stiffness) performed by incrementing the displacement of a control node, a force-displacement equivalent SDoF response of the structure (referred to as displacement-based pseudo-pushover in [16] and hereinafter) is obtained. Modal superposition can be also implemented to account for higher-modes contributions. DBA algorithms can also be applied for analysing the longitudinal seismic response of straight continuous-deck multi-span bridges. Since the superstructure can be typically assumed axially rigid in the longitudinal direction, the seismic response of the bridge can be represented by the response of the resisting substructure members working in parallel. This process is simpler than in the transverse direction, as it requires no iterations. Past studies describe the DBA algorithms for multi-span bridges in the longitudinal direction [5].

Starting from the displacement-based pseudo-pushover, two strategies for the seismic response analysis are adopted to obtain fragility curves.

DBA+CSM

The first strategy (referred to as DBA+CSM hereafter) is based on the use of the so-called capacity spectrum method (CSM) [17]. The CSM is used as an approximate strategy to compute the seismic performance of the bridge under a given seismic action represented by a ground-motion response spectrum. The hysteretic dissipation related to the cyclic response of the structure is accounted for by means of spectral reduction factors and equivalent viscous damping coefficients. The method leads to the direct calculation of the seismic demand in terms of the equivalent SDoF displacement. In any case, other EDPs can be calculated by recording their variation as the effective displacement changes during the pseudo pushover. Further explanations on the use of the CSM with record-specific spectra are reported in [17]. Considering the previous applications, the DBA+CSM is proved to be more accurate for bridges for which the seismic response is governed by the first mode of vibration and for which the damage generated by the ground motion only slightly modifies the first modal shape (i.e., the elastic first mode shape is similar to the inelastic one computed with secant stiffness properties). In addition, the approximations of the method are related to the simplified formulations for the calculation of the equivalent cantilever response of the piers and to the equivalent damping formulations adopted for hysteretic damping.

The DBA+CSM can be applied to generate the seismic demand dataset of the investigated bridge subjected to a suite of ground-motion spectra. In this way, $[edp, im]_j$ cloud data are

computed. This enables fragility analysis using the chosen functional form for the probabilistic seismic demand model and DS thresholds.

DBA+GP

The second strategy (referred to as DBA+GP) is based on the surrogate probabilistic seismic demand models (PSDMs) based on a Gaussian Process (GP) regression developed in [18]. Such surrogate models are developed based on a training dataset composed of 10'000 SDoF systems defined based on wide ranges of the following input parameters: hysteresis model "$hyst$" (i.e., kinematic hardening, modified Takeda, modified Sina, flag shape); secant-to-yielding period T; the yield shear strength, normalised to the total weight, or shear ratio f_y; the hardening ratio h. Each SDoF in the dataset is analysed to derive a cloud of points in the EDP vs IM space. The selected EDP in this study is the ductility demand μ. The selected IM is the pseudo-spectral acceleration at the SDoF period, normalised to the yield base shear coefficient, $R = SA/f_y$. Each SDoF is subjected to 100 natural (i.e. recorded) ground motions selected from the SIMBAD database [19], and scaled to obtain responses in the range [1, 6] of the SDoF ductility demand. For each case, a bi-linear PSDM is defined according to Eq. 6, and its parameters (a, σ) are used as training points for a GP regression. The adopted IM is the spectral acceleration ratio R_{IM}.

The resulting surrogate model allows deriving the parameters (a, σ) of an SDoF system based on the input parameters ($hyst, T, f_y, h$). By also specifying different DS thresholds in terms of ductility capacity μ_{DS_i}, it is finally possible to obtain a set of fragility curves. According to the properties of the adopted PSDM, lognormal fragility curves for each DS, representing the DSs' exceeding probability $F_{DS_i} = P(\mu \geq \mu_{DS_i}|R)$, are completely specified by their median η_{DS} and logarithmic standard deviation β (simply called dispersion), which are specified in Equation (8) both for the elastic and inelastic ranges. It is worth mentioning that collapse cases (corresponding to ground motions leading to dynamic instability of the analysis or exceedance of a conventional 10% drift threshold) are not expected since the SDoF systems are only subjected to pre-peak ductility demand levels.

$$\mu_{DS_i} \leq 1;\ \begin{cases}\eta_{DS_i} = \mu_{DS_i} \\ \beta = 0\end{cases} \qquad \mu_{DS_i} > 1;\ \begin{cases}\eta_{DS_i} = \dfrac{\mu_{DS_i} - 1}{a} + 1 \\ \beta = \sigma\end{cases} \tag{8}$$

3 PARAMETRIC ANALYSIS

3.1 Case-study bridge realisations

The dataset of case studies for the parametric analysis is composed of 18 realisations of straight, continuous-deck, RC bridges with single-column piers. Pinned superstructure-substructure connections are considered in the transverse direction. In the longitudinal direction, pinned supports are placed on the piers, while sliders are considered on the abutments. No strength limits for the pinned supports are considered. The superstructure is composed of three V-shaped pre-stressed beams. The main geometric parameters of the case-study bridges are shown in Figure 1. The different bridge geometries include with two, four, or six 35m-long spans. Pier heights of 7m, 14m and 21m are adopted to define regular and irregular geometric configurations. As an example, the case study labelled as B132 is a four-span bridge with an 8m-, 20m- and 15m-tall piers.

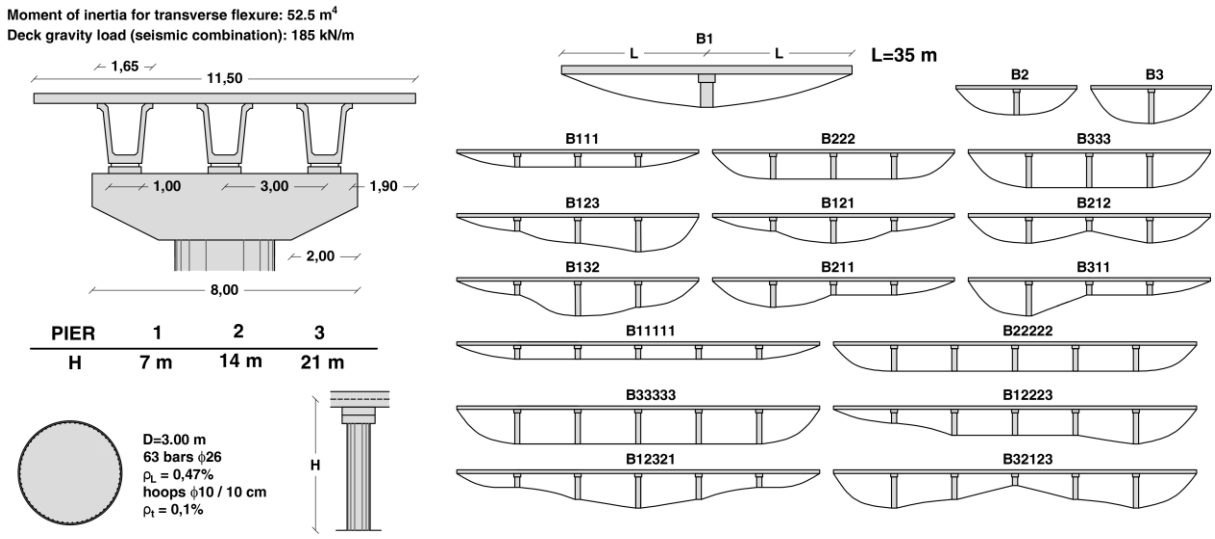

Figure 1. Parametric case-study bridges.

3.2 Modelling and analysis assumptions

Numerical models of the presented bridge realisations are carried out by using the Opensees framework [20], following the modelling strategy shown in [5]. In detail, the superstructure is modelled as an elastic frame considering a 5 m-discretisation for assigning the structural and non-structural tributary masses. The superstructure is connected to the substructure components through a set of two-node links [5] simulating the eccentricity in the transverse direction of the beam axes with respect to the axis of the piers. The nonlinear response is lumped in the piers which are modelled as *ForceBeamColumn* elements in which a fibre discretisation of the cross-section is adopted. The *Concrete01* and *Steel01* materials are used for concrete and steel fibres. Piers are fixed at their base, while abutments are simulated as fixed supports.

The analytical iterative DBA calculations are performed via programming routines implemented in MATLAB. The force-displacement laws to be assigned to the inelastic supports are calculated by using sectional moment-curvature analysis and applying estimations of the equivalent cantilever heights of the piers H_{eff}. This latter is assumed as the distance between the pier base and the centre of mass of the pier cap for the response in longitudinal direction (H_p). For the response in transverse direction, H_{eff} is computed via Equation (10) in which m_{pc}. m_p and m_{sup} are the masses of the pier cap, the pier and the tributary mass of the superstructure; H_d is the height of the centre of mass of the superstructure. The equivalent viscous damping of the pier ξ_{eq} is calculated through the ductility-based formulation proposed by Priestley et al. [21] reported in Equation (10) which is applied for each pier. For other formulations involved in the DBA approaches, readers can refer to references [5, 16]. Displacement-based pseudo pushover for the case-study bridge realisations are reported in [16].

$$H_{eff} = \frac{(m_{pc} + 0.3m_p)H_p + m_d H_d}{m_{eff}}; m_{eff} = 0.3m_p + m_{pc} + m_{sup} \tag{9}$$

$$\xi_{eq} = 0.05 + 0.444\left(\mu - 1/\pi\mu\right) \tag{10}$$

In this study, the DBA+CSM is carried out according to the iterative algorithm presented in [22] which allows for the consideration of higher modes and modal damping. The record-to-record variability for fragility analysis is considered by using a suite of 100 natural, unscaled ground-motion sets extracted from the SIMBAD database [19]. Each ground-motion record is

applied separately in the transverse and longitudinal direction. To define the ground-motion suite, the 100 records having the highest peak ground acceleration (PGA) in the horizontal direction and soil type B and C within the SIMBAD database are selected. The selected records are characterised by PGA ranging between 1.77g and 0.10g. The NLTHA are carried out by assuming a tangent-stiffness damping strategy and a damping equal to 5% is assigned to all the modal shapes.

3.3 Assumptions of the strategies for fragility and loss assessment

This subsection lists the assumptions adopted for each considered loss-assessment strategy for probabilistic seismic demand models and DS thresholds. For the DBA+CSM and NLTHA approaches, both power-law and bilinear relationships are implemented in fitting PSDMs. Considering that a system-level loss assessment is carried out, probabilistic seismic demand models and fragility curves are computed by using the displacement demand of the equivalent SDoF system, Δ_{EDP}^{SDoF}, as an EDP. DS thresholds in terms of Δ_{DS}^{SDOF} are calibrated consistently with the attainment of curvature thresholds (Table 1). To do so, displacement-based pseudo pushover analyses are carried out according to [16], for each of bridge realisations and analysis direction. In Table 1, the considered curvature DSs indicate: 1) yielding of steel bars, 2) spalling of concrete cover layer, 3) fracture of the transverse reinforcement or excessive deformation of the longitudinal bars, 4) concrete core crushing.

Table 1. Damage state thresholds and damage-to-loss-ratios (ε_c: concrete compression strain the cover layer, ρ_v and f_{yh} are the geometric percentage and yielding strength of transverse reinforcements, f'_{cc} is the compression strength of the confined concrete, ε_{su} is the ultimate deformation of longitudinal steel bar).

	DS1	DS2	DS3	DS4
Pier curvature ($\boldsymbol{\chi_{DS}}$)	χ_y	$\chi(\varepsilon_c = 0.004)$	$\chi\left(\varepsilon_c = 0.004 + \frac{1.4\,\rho_v f_{yh}\varepsilon_{su}}{f'_{cc}}\right), 0.6\varepsilon_{su})$	χ_u
DLR	0.03	0.08	0.25	1.00

To apply the DBA-GP, the displacement-based pseudo pushover curves computed for each bridge and each analysis direction are first bi-linearised to derive the equivalent SDoF parameters reported in Table 2. For some of the considered bridge realisations (highlighted in the Table 2), the combination of those parameters is out of the range of the training dataset and, therefore, the algorithm is called to perform extrapolations which can cause loss of accuracy. A Modified Takeda "Thin" model is used to characterise equivalent SDoF hysteretic dissipation (characterised by the parameter $\alpha = 0.5$). The DS thresholds adopted in this case are defined based on the previously mentioned Δ_{DS}^{SDOF} corresponding to reaching of curvature limits for bridge piers.

Table 2. Equivalent single-degree-of-freedom parameters of the analysed bridges. The field "Extr" indicates if extrapolation is carried out or not (Y: Yes, N: No) considering the training dataset.

	Transverse direction					Longitudinal direction				
Name	T	f_y	h	μ_c	Extr.	T	f_y	h	μ_c	Extr.
B1	0.23	1.48	0.48	3.48	Y	0.51	0.34	0.02	2.85	N
B2	0.31	3.17	0.89	3.69	Y	1.40	0.16	0.02	3.61	N
B3	0.33	6.69	0.97	3.72	Y	2.61	0.10	0.02	3.70	Y
B111	0.34	0.65	0.07	3.00	Y	0.43	0.49	0.02	2.85	N
B222	0.84	0.43	0.34	3.12	Y	1.17	0.22	0.01	3.61	N
B333	1.16	0.52	0.64	3.13	Y	2.19	0.15	0.02	3.70	Y

B123	0.67	0.43	0.32	1.95	Y	0.68	0.19	0.16	2.85	N
B121	0.46	0.52	0.17	2.94	N	0.51	0.34	0.08	2.85	N
B212	0.46	0.33	0.20	3.22	N	0.66	0.20	0.22	2.85	N
B132	0.68	0.36	0.41	2.18	Y	0.68	0.19	0.16	2.85	N
B211	0.42	0.55	0.24	2.41	N	0.51	0.34	0.08	2.85	N
B311	0.43	0.52	0.25	2.40	N	0.52	0.33	0.04	2.85	N
B11111	0.35	0.50	0.07	3.24	N	0.41	0.53	0.02	2.85	N
B22222	0.99	0.30	0.12	3.13	N	1.12	0.24	0.01	3.61	N
B33333	1.68	0.24	0.28	3.13	Y	2.10	0.16	0.01	3.70	Y
B12223	0.95	0.32	0.23	2.46	N	0.76	0.15	0.32	2.85	Y
B12321	0.85	0.39	0.22	1.90	N	0.60	0.24	0.15	2.85	N
B32123	0.66	0.22	0.24	2.47	N	0.79	0.14	0.27	2.85	N

For consistency, the adopted IM is the SA in all the adopted strategies. To complete the risk assessment, hazard curves related to the city of L'Aquila (Italy) are used, directly adopting the Italian hazard model [23], consistent with the Italian bridge design code.

4 DISCUSSION OF RESULTS

In this section, the accuracy of the simplified loss assessment procedures is discussed by considering the two different functional forms adopted for the probabilistic seismic demand models. The comparisons are carried out accounting for the fragility analysis results (i.e. median fragility and dispersion) and the EAL.

With reference to the power-law functional form, DBA+CSM and NLTHA are compared. Figure 2 illustrates the relative errors between the median fragility and dispersion computed by using the two approaches (i.e. $[X_{DBA+CSM} - X_{NLTHA}]/X_{NLTHA}$ where X can be the median or the dispersion). The median fragility predicted by DBA+CSM presents errors lower than 25% compared to NLTHA. The average of the absolute errors is equal to 10% and 15% considering DS1 and DS4 in longitudinal direction. Generally, in the transverse direction, the DBA+CSM underestimates the median fragility with respect to NLTHA with errors lower than 20%. Although those results demonstrate a satisfying accuracy of the DBA+CSM in predicting the fragility median, the errors on fragility dispersion are significantly higher. In the transverse direction, DBA+CSM overestimates the fragility dispersion in case of bridge realisations having 14m- and 21m-tall piers, whereas the contrary is observed for bridges whose seismic response is governed by short piers. Further analyses should be carried out to better describe the drivers of those errors, especially referring to the SDoF simplification.

The influence on EAL of the abovementioned discrepancies can be quantified by observing Figure 3. As a general outcome, Figure 3 shows that the EAL values are lower for the longitudinal direction with respect to the transverse one. This is a useful remark to consider when developing a simplified loss-based design framework which considers the response of the bridge in the critical direction as proposed by Gentile and Calvi for buildings [2]. Figure 3 also shows that, as expected, short piers introduce a higher bridge vulnerability with respect to taller piers. Table 3 reports the relative errors on EAL estimated by DBA+CSM and NLTHA. In the longitudinal direction, the DBA+CSM provides satisfying accuracy with respect to NLTHA. Particularly, in this case, it overestimates the NLTHA-based EAL with an average error equal to 20% within the case-study dataset. Higher errors are associated with bridge realisations whose DS is governed by tall piers (i.e. B3, B333, B33333). However, such case studies are associated with negligible EAL values (i.e., lower than 10^{-5}) and, therefore, such relative errors are not deemed unsatisfactory, since they correspond to particularly low errors in absolute

terms. In the transverse direction, the overestimations of the DBA+CSM are more significant, despite of the accuracy in predicting the fragility median. This result is likely caused by the relevant overestimation of the fragility dispersion by the DBA+CSM inducing overestimations in the probability of damage for low IM values which are characterised by a relevant annual probability of exceedance. In both directions, the DBA+CSM produces EAL estimations which are on the safe side compared to NLTHA. This would be a desirable feature of an approximate loss-based design procedure.

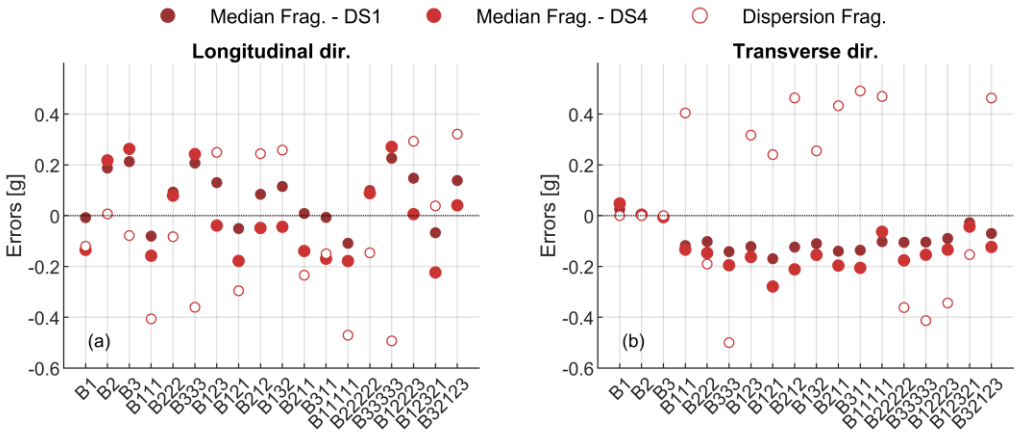

Figure 2. Errors on the medians (DS1 and DS4) and dispersion in fragility curves between NLTHA and DBA+CSM considering a power-law response model: a) longitudinal and b) transverse direction.

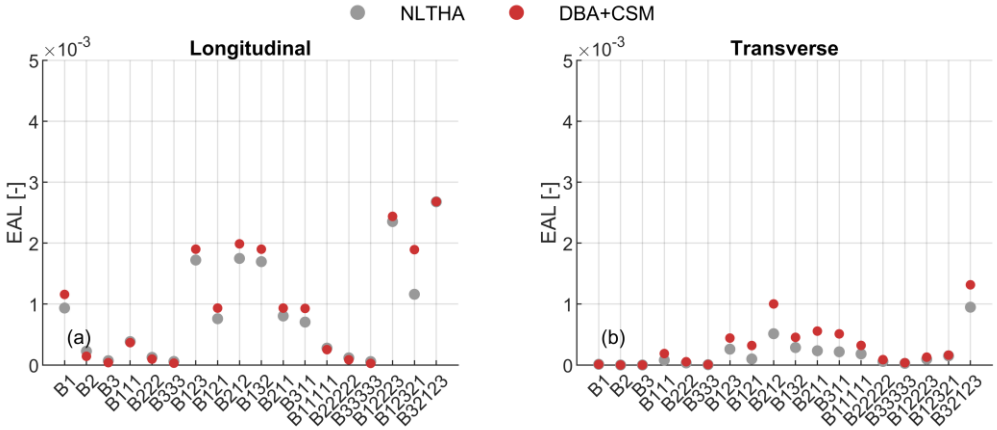

Figure 3. Expected Annual Losses computed by DBA+CSM and NLTHA considering a power-law response model: a) longitudinal and b) transverse direction.

Table 3. Relative errors [-] for the expected annual loss $(EAL_{DBA+CSM} - EAL_{NLTHA})/EAL_{NLTHA}$.

	B1	B2	B3	B111	B222	B333	B123	B121	B212
Long.	0.24	-0.37	-0.45	-0.05	-0.23	-0.48	0.10	0.23	0.14
Transv.	-0.12	-0.10	1.88	1.34	0.59	0.55	0.70	2.22	0.95

	B132	B211	B311	B11111	B22222	B33333	B12223	B12321	B32123
Long.	0.12	0.16	0.32	-0.09	-0.27	-0.54	0.04	0.63	0.00
Transv.	0.59	1.38	1.36	0.76	0.51	0.41	0.35	0.08	0.39

The following discussion assesses the accuracy of the simplified loss assessment procedures if a bilinear functional form is assumed for the PSDM. Figure 4 reports the relative errors on fragility median and dispersion for DS4 by using DBA+CSM (red markers) and DBA+GP (blue markers) with respect to NLTHA. Figure 4 shows that the errors of the DBA+CSM increase (for both fragility median and dispersion) if a bilinear model is used, compared to using a power law (Figure 2). This is because the fitting of the bilinear model only considers inelastic cases where the DBA+CSM inaccuracy increases, with respect to the case of a power-law model, in which both elastic and inelastic cases are used for the fitting process. The DBA+GP is, on average, more accurate than the DBA+CSM considering the fragility medians. The average absolute error is equal to 20% and 5% in the longitudinal and transverse directions, respectively. However, the accuracy in computing the fragility dispersion is particularly low. This result could be related to the SDoF simplification (neglecting higher modes and modifications of modal shapes in the inelastic field) on which the GP surrogate model is trained, which could be inaccurate for the considered bridge realisations. As per the above discussion, this aspect requires further investigation.

Figure 5 presents the EAL computed with the NLTHA, DBA+GP and DBA+CSM if a bilinear model is used. Since the fragility curves related to DS1 (computed without the need for performing any response analysis) are identical for all the considered procedures, the discrepancies in the EAL depend only on DS2 to DS4. The results show that the DBA+GP leads to a strong underestimation of NLTHA-based losses in both longitudinal and transverse direction. This inaccuracy is clearly derived by the underestimation in fragility dispersion provided by DBA+GP compared to NLTHA shown in Figure 4. In the longitudinal direction, the DBA+CSM outperforms DBA+GP, leading to average errors on EAL equal to -20% and -16% for four-span and six-span bridges. Conversely, in the transverse direction, DBA+CSM leads to severe loss overestimations for most of the four-span bridges.

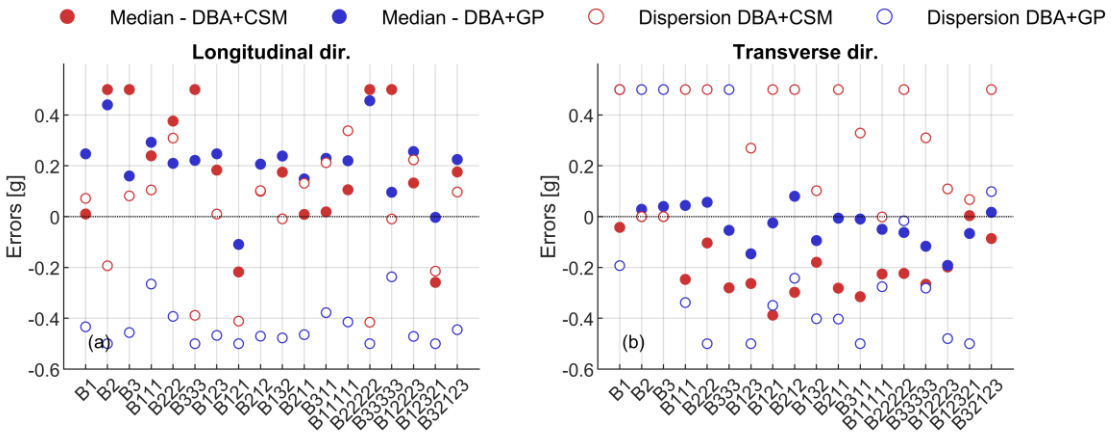

Figure 4. Errors on the median and dispersion (DS4) in fragility curves between NLTHA, DBA+CSM, DBA+GP considering a bilinear response model: a) longitudinal and b) transverse direction.

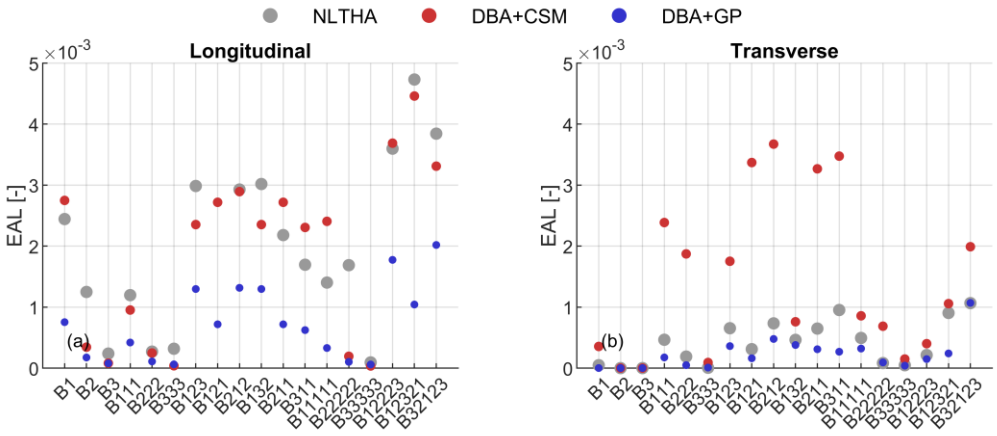

Figure 5. Expected Annual Losses computed by NLTHA, DBA+CSM and DBA+GP considering a bilinear response model: a) longitudinal and b) transverse direction.

The discrepancies between EAL computed by using a power-law or bilinear model can be observed by comparing Figure 3 and Figure 5. In all the analysed cases, the use of a bilinear model leads to a relevant overestimation with respect to a power-law model. If an NLTHA is used as a response analysis, Table 3 shows that the EAL computed by using a power-law model are, on average, 40% and 50% lower compared to the case in which a bilinear model is used. This result motivates the need for the identification of the optimal strategy by performing comparisons with respect to other analysis approaches (e.g. multi-stripe fragility analyses) not relying on specific functional forms for probabilistic seismic demand models.

Table 4. Discrepancies of the expected annual loss computed by using a power-law or a bilinear model and NLTHA ($EAL^{PL}_{NLTHA}/EAL^{BL}_{NLTHA}$).

	B1	B2	B3	B111	B222	B333	B123	B121	B212
Long.	0.38	0.18	0.30	0.32	0.46	0.18	0.58	0.11	0.60
Transv.	0.25	~0.00	~0.00	0.17	0.18	0.85	0.40	0.32	0.70

	B132	B211	B311	B11111	B22222	B33333	B12223	B12321	B32123
Long.	0.56	0.37	0.42	0.20	0.07	0.61	0.65	0.25	0.70
Transv.	0.62	0.36	0.23	0.37	0.71	0.56	0.45	0.17	0.89

5 REMARKS AND FUTURE DEVELOPMENTS

As the first step towards practical loss-based design for multi-span bridges, this study tests the accuracy of simplified loss assessment strategies. A set of 18 case-study continuous-deck bridges with single-column piers, imagined in a high-seismicity site, is analysed. For each of them, a benchmark estimation of the expected annual loss is obtained running non-linear time-history analyses (NLTHA) of refined multi-degree of freedom models. Such estimates are independently obtained with two simplified alternative strategies based on analytical, displacement-based pseudo pushover analysis. The first uses the capacity spectrum method (DBA+CSM), whereas the second involves surrogate probabilistic seismic demand model based on a gaussian process regression (DBA+GP). This sensitivity analysis also tests the impact of two different assumptions regarding the adopted functional form for the probabilistic seismic demand model: a power-law and a bilinear model.

DBA+CSM appears promising for future loss-based design applications, while adopting DBA+GP would require challenging some of its simplified assumptions. Indeed, using a power-

law model, it produces loss estimates with satisfying accuracy in the analysis in longitudinal direction, overestimating NLTHA-based expected annual losses by an average of 20%. The errors increase significantly in the transverse direction. However, these could be less critical from a design standpoint based on the critical direction because the losses in the transverse direction are lower than those calculated in the longitudinal direction. In contrast, using a bilinear model is used, DBA+GP significantly underestimates NLTHA-based losses in both longitudinal and transverse directions. Although in the longitudinal direction the DBA+CSM outperforms DBA+GP, it leads to severe loss overestimations in the transverse direction for many cases. These results indicate both the simplified strategies, with the current set of assumptions, fail to consistently predict NLTHA-based estimations.

As a result, further research is needed to refine the assumptions of the above simplified loss-assessment strategies and develop a robust loss-based design framework for bridges. Indeed, the results show that losses computed by using a power-law model are in average 40% and 50% lower than those from a bilinear model. Comparative studies with fragility analysis approaches (e.g. multi-stripe fragility analyses) not relying on specific functional forms for probabilistic seismic demand models, are recommended. Additionally, future investigations should quantify the limitations of a system-level loss computation, as used in this study, against more detailed component-based loss estimations employing local parameters in fragility analysis.

REFERENCES

[1] Performance-Based Seismic Engineering. Structural Engineers Association of California. SEAOC Vision 2000 Committee, 1995.

[2] R. Gentile, G. M. Calvi, Direct loss-based seismic design of reinforced concrete frame and wall structures, *Earthquake Engineering and Structural Dynamics*, **52**, no. 14, 2023, doi: 10.1002/eqe.3955.

[3] R. Gentile, C. Galasso, Simplicity versus accuracy trade-off in estimating seismic fragility of existing reinforced concrete buildings, *Soil Dynamics and Earthquake Engineering*, 2021, doi: 10.1016/j.soildyn.2021.106678.

[4] Federal Emergency Management Agency (FEMA), Hazus Earthquake Model Technical Manual - Hazus 5.1. Federal Emergency Management Agency (FEMA), 2022. [Online]. Available: https://www.fema.gov/sites/default/files/documents/fema_hazus-earthquake-model-technical-manual-5-1.pdf

[5] A. Nettis, D. Raffaele, G. Uva, Seismic risk-informed prioritisation of multi-span RC girder bridges considering knowledge-based uncertainty, *Bulletin of Earthquake Engineering*, 2023, doi: 10.1007/s10518-023-01783-y.

[6] M. A. Zanini, F. Faleschini, C. Pellegrino, Probabilistic seismic risk forecasting of aging bridge networks, *Engineering Structures*, **136**, 219–232, 2017, doi: 10.1016/j.engstruct.2017.01.029.

[7] Federal Emergency Management Agency (FEMA), Multi-hazard loss estimation methodology technical manuals and user's manuals for the earthquake advanced engineering building module (AEBM), the earthquake model, the flood model, and the hurricane model. FEMA, National Institute of Building Sciences., Washington DC, 2012.

[8] C. Perdomo, A. Abarca, R. Monteiro, Estimation of Seismic Expected Annual Losses for Multi-Span Continuous RC Bridge Portfolios Using a Component-Level Approach, *Journal of Earthquake Engineering*, **26**, no. 6, 2985–3011, 2022, doi: 10.1080/13632469.2020.1781710.

[9] A. Abarca, R. Monteiro, G. J. O'Reilly, Simplified methodology for indirect loss–based prioritization in roadway bridge network risk assessment, *International Journal of Disaster Risk Reduction*, **74**, no. December 2021, 102948, 2022, doi: 10.1016/j.ijdrr.2022.102948.

[10] Y. Dong, D. M. Frangopol, Risk and resilience assessment of bridges under mainshock and aftershocks incorporating uncertainties, *Engineering Structures*, **83**, 198–208, 2015, doi: 10.1016/j.engstruct.2014.10.050.

[11] F. Jalayer, H. Ebrahimian, A. Miano, G. Manfredi, H. Sezen, Analytical fragility assessment using unscaled ground motion records, *Earthquake Engineering and Structural Dynamics*, **46**, no. 15, 2639–2663, 2017, doi: 10.1002/eqe.2922.

[12] G. J. O'Reilly, Seismic intensity measures for risk assessment of bridges, *Bulletin of Earthquake Engineering*, 2021, doi: 10.1007/s10518-021-01114-z.

[13] G. J. O'Reilly, R. Monteiro, Probabilistic models for structures with bilinear demand-intensity relationships, *Earthquake Engineering and Structural Dynamics*, 2019, doi: 10.1002/eqe.3135.

[14] J. W. Baker, Efficient analytical fragility function fitting using dynamic structural analysis, *Earthquake Spectra*, 2015, doi: 10.1193/021113EQS025M.

[15] O. B. Şadan, L. Petrini, G. M. Calvi, Direct displacement-based seismic assessment procedure for multi-span reinforced concrete bridges with single-column piers, *Earthquake Engineering and Structural Dynamics*, 2013, doi: 10.1002/eqe.2257.

[16] R. Gentile, A. Nettis, D. Raffaele, Effectiveness of the Displacement-Based seismic performance Assessment for continuous RC bridges and proposed extensions, *Engineering Structures*, 2020, doi: 10.1016/j.engstruct.2020.110910.

[17] A. Nettis, R. Gentile, D. Raffaele, G. Uva, C. Galasso, Cloud Capacity Spectrum Method: accounting for record-to-record variability in fragility analysis using nonlinear static procedures, *Soil Dynamics and Earthquake Engineering*, 2021, doi: 10.1016/j.soildyn.2021.106829.

[18] R. Gentile, C. Galasso, Surrogate probabilistic seismic demand modelling of inelastic single-degree-of-freedom systems for efficient earthquake risk applications, *Earthquake Engineering and Structural Dynamics*, **51**, no. 2, 2022, doi: 10.1002/eqe.3576.

[19] C. Smerzini, C. Galasso, I. Iervolino, R. Paolucci, Ground motion record selection based on broadband spectral compatibility, *Earthquake Spectra*, **30**, no. 4, 1427–1448, 2014, doi: 10.1193/052312EQS197M.

[20] F. McKenna, OpenSees: A framework for earthquake engineering simulation, *Computing in Science and Engineering*, 2011, doi: 10.1109/MCSE.2011.66.

[21] M. J. N. Priestley, G. M. Calvi, M. J. Kowalsky, *Displacement-based seismic design of structures*. IUSS Press, Pavia, Italy, 2007.

[22] A. Nettis, P. Iacovazzo, D. Raffaele, G. Uva, J. M. Adam, Displacement-based seismic performance assessment of multi-span steel truss bridges, *Engineering Structures*, **254**, no. July 2021, 113832, 2022, doi: 10.1016/j.engstruct.2021.113832.

[23] M. Stucchi, C. Meletti, V. Montaldo, H. Crowley, G. M. Calvi, E. Boschi, Seismic hazard assessment (2003-2009) for the Italian building code, *Bulletin of the Seismological Society of America*, **101**, no. 4, 1885–1911, 2011, doi: 10.1785/0120100130.